ELSEVIER

Journal of Power Sources 54 (1995) 416–420

JOURNAL OF POWER SOURCES

Influence of the composition of lithium-based alloys, non-aqueous electrolytes and cycling conditions on the anode properties

E.M. Shembel [a,*], I.M. Maksyuta [a], L.I. Neduzhko [a], A.I. Belosokhov [b], A.F. Naumenko [b], V.V. Rozhkov [b]

[a] *Ukrainian State Chemical Technology University, 320005 Dniepropetrovsk, Ukraine*
[b] *Chemical Concentrates Plant, 630038 Novosibirsk, Russian Federation*

Abstract

The reversible work of a lithium-based anode in non-aqueous electrolytes of different compositions has been investigated. The electrochemical properties of anodes of Li, binary Li–Al alloys, ternary Li–Al–Cd, Li–Al–Si, Li–Al–Bi alloys were compared. The concentration range of aluminium in the alloys was used in accordance with a binary constitutional diagram. In a series of binary alloys with an Al content 5, 16.8, and 22.5 mass%, in the process of anode 'ageing', the alloy containing 16.8 mass% Al is passivated to a greater extent. Hence, cycling efficiency of lithium deposits changed. The increase in charge-current density and the discharge-current density decrease raise the efficiency of lithium deposits. Comparison of the results of impedance measurements and galvanostatic cycling showed that the efficiency of galvanostatic cycling is higher when the active component of impedance is lower. The polarization of cathode process (deposition) and anode process (dissolution) decreases significantly in a series of lithium anodes: anodes on the basis of binary Li–Al alloys and anodes based on ternary alloys. Lithium insertion into the structure of ternary alloys proceeds considerably easier than into lithium or binary lithium–aluminium alloy structures. It may be conditioned by the binary alloy passivation in the electrolyte and by the less passivating film resistance on the ternary alloys.

Keywords: Lithium-based alloys; Electrolytes; Cycling; Anodes

1. Introduction

The efficiency of power sources with non-aqueous electrolytes and lithium anodes, and the important parameters, such as specific power, self-discharge, voltage delay at current turning-on, the efficiency of charge/discharge cycles and cycle life, are determined by the properties of film-passivating lithium surface.

Analysis of literature data and our previous earlier work show that the electrochemical behaviour of lithium electrodes is conditioned by non-aqueous electrolyte compositions, electrode prehistory (lithium electrode 'ageing' before the beginning of investigations or preliminary electrochemical dissolving lithium surface), and conditions of deposition.

The modification of the anode surface is based on the surface or volume of the lithium alloys. In most cases, binary lithium–aluminium alloys are the basis of such alloys [1–3]. The alloys of a more complex composition containing two or three metals besides lithium [5,6] have called for the attention of researchers and designers of batteries. The aim of the present work is to study the electrochemical behaviour of lithium anodes on basis of the different alloys. The concentration range of aluminium in binary alloys did not exceed 25 mass%. Silicon, cadmium or bismuth are introduced into the alloy as the third component. The dynamic characteristics of anode passivation, lithium deposition and deposit dissolution were investigated depending on the prehistory of the base of the alloys and their deposit. The interaction between the passivation rate of the base surface and cycling efficiency of the deposit on different lithium alloys has been studied. $LiClO_4$, $LiBF_4$, $LiAsF_6$ and $LiPF_6$ solutions were used as non-aqueous electrolytes in propylene carbonate, dimethyl ether of diethyleneglycol, and dimethoxyethane solvents. Some of the non-aqueous electrolytes were prepared under the supervision of the Institute of Railway Transport Engineers, Dniepropetrovsk, Ukraine.

---

[*] Corresponding author.

SSDI 0378-7753(94)02114-I

2. Experimental

All operations concerning the preparation of the electrode and the electrochemical experiments were carried out in an argon-filled dry glove box. The water content in the electrolytes did not exceed 0.02%. Two kinds of anode were produced from the investigated materials. The first one, a cylinder was pressed into a glass tube. The end (0.12 cm^2) is the operating surface. A steel wire inserted into the electrode body was used as current collector. In the second one, the anode material was pressed on to a flat grid of stainless steel or nickel. The cathodic deposition of lithium and its anodic dissolution was carried out in the regime of galvanostatic polarization, and the potential–time curves were fixed. Galvanostatic measurements were carried out in a three-electrode cell, lithium served as reference and auxiliary electrodes.

Impdedance measurements were performed in a two-electrode cell in order to have information on the properties of passivating film formed on the anode surface as well as on the lithium deposit surfaces. A platinized platinum plate sealed in glass was used as auxilliary electrode. In the electrochemical cell, the auxiliary electrode was placed horizontally under the lithium electrode. The geometric surface of the auxiliary electrode exceeded that of the surface of electrode studied by a factor of 50. The capacity measurements of the lithium/non-aqueous interface near the equilibrium potential were carried out with the help of an a.c. bridge in a frequency range from 80 to 200 kHz. The amplitude of alternating voltage was 5 mV. The measurements were carried out according to a step-by-step substitution scheme.

The preparation of the electrode surface, i.e., its prehistory, has a great influence on the behaviour of lithium electrode. The investigations were performed on an electrode with a surface renewed by layer cutting, anodic dissolution, as well as on the electrode after lithium deposition. For the study of the impedance characteristics of electrodes with different prehistory glass cells with four electrodes were used. In such a system a cell for galvanostatic investigations was integrated into a cell for impedance measurements. It includes lithium reference and auxilliary electrodes, auxilliary platinum electrode and working electrode on the basis of lithium or its alloys.

3. Results and discussion

3.1. Resistance of the passivating film on Li–Al alloys

Circular arc of the lithium electrode impedance in non-aqueous electrolyte appears as a semi-circle. The ohmic resistance of the passivating film on the electrode surface [7,8] can be determined by the value of the intercept on the *x–y* axes. In Fig. 1, impedance characteristics of the electrodes on basis of different lithium–aluminium alloys are presented. The impedance of the passivating film on freshly cut electrode surfaces depends little on the alloy composition: 6 Ω cm^2 (5 mass% Al), 8 Ω cm^2 (16.8 mass% Al) and 10 Ω cm^2 (22.5 mass% Al). In the process of electrode 'ageing', the electrode with an Al content of 16.8 mass% Al is passivated to a greater extent than two other investigated alloys (Fig. 1, Table 1). Thus, in a series of alloys with an aluminium content of 5, 16.8 and 22.5 mass%, respectively, the rate of alloy passivation versus time passes through a maximum. At the same time, a further increase in the aluminium content is unreasonable in terms of anode volume use. Minimum passivation is observed when the alloy contains 5 mass% Al. On an electrode without aluminium, the passivation rate is higher than on the investigated alloys (Table 1).

3.2. Effect of the substrate passivation on a cycling process

Cycling results of electrodes on the basis of different alloys were studied. The galvanostatic lithium deposition/dissolution curves are shown in Fig. 2. The results obtained on the substrate passivated to different extents were compared before lithium deposition. The curves

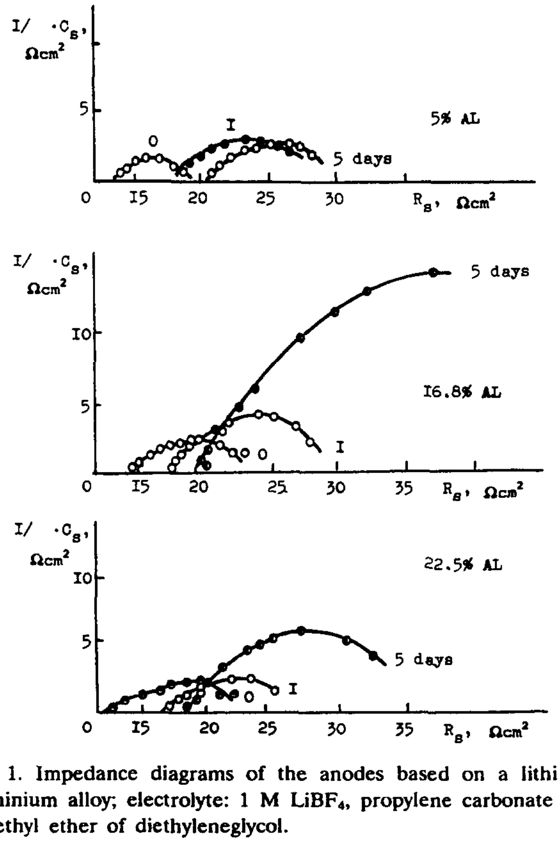

Fig. 1. Impedance diagrams of the anodes based on a lithium–aluminium alloy; electrolyte: 1 M LiBF$_4$, propylene carbonate and dimethyl ether of diethyleneglycol.

Table 1
The resistance of lithium-based anode/non-aqueous electrolyte interface determined from impedance measurements

Electrode type	Time of 'ageing' (24 h)	Interfacial resistance (Ω)
Electrolyte: propylene carbonate, dimethoxyethane, 1 M lithium perchlorate		
Metallic lithium	1	62
Lithium–aluminium alloy, 5 mass% Al	1	32
Electrolyte: propylene carbonate, diglym, 1 M lithium tetrafluoroborate		
Metallic lithium	1	70
Lithium–aluminium alloy, 5 mass% Li	6	10
Lithium–aluminium alloy, 16.8 mass% Al	1 5	12 40
Lithium–aluminium alloy, 22.5 mass% Al[a]	1 5	10 18

[a] Value obtained by extrapolation.

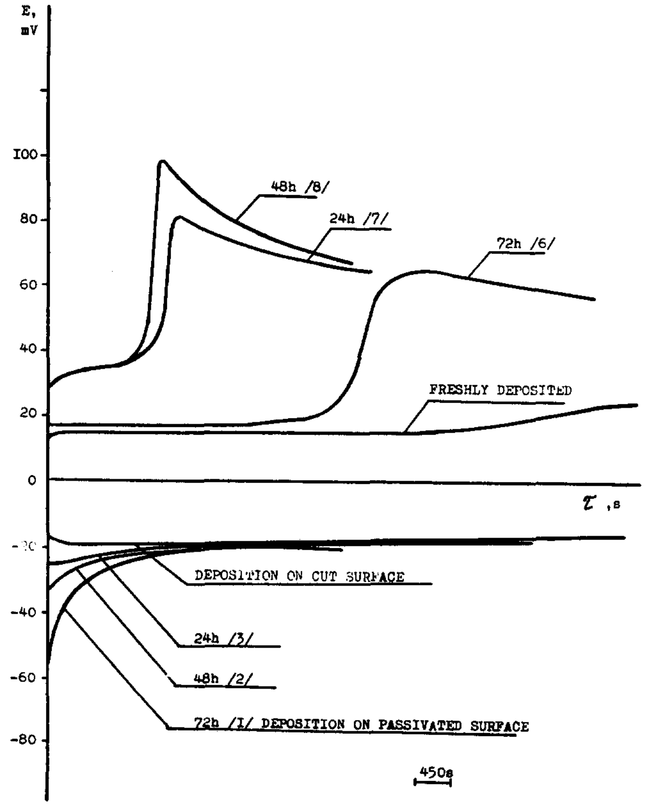

Fig. 2. Galvanostatic curves of lithium deposition on a lithium–aluminium alloy depending on the time of a substrate 'ageing'. Electrolyte: 1 M LIBF$_4$, propylene carbonate–dimethyl ether of diethyleneglycol. Charge current = 0.5 mA/cm^2. Discharge current of deposit: 0.5 mA/cm^2 (curves (5), (6)), 1 mA/cm^2 (curves (7), (8)). Figures on curves indicated the time of preliminary passivation of the substrate.

located in the lower part of the Figure correspond to the cathodic deposition of lithium on a substrate passivated in electrolyte for different periods of time. Curve (1) in Fig. 2 corresponds to the lithium deposition on a freshly cut and then anodically treated lithium surface. In the case of lithium deposition on passivated substrate, cathodic polarization is larger (curves (1), (2), and (3) of Fig. 2) in the initial stage, then it gradually decreases. Stationary potential of lithium deposition is practically independent of the extent of substrate passivation. In the upper part of Fig. 2 *E*-curves correspond to the anodic dissolution of fresh lithium deposits obtained on the 'aged' electrode surface.

The curves of lithium deposit dissolution have two sections. The initial section corresponds to the dissolution of the lithium deposit itself which has an extended surface. The second one corresponds to the base dissolution. The deposit efficiency was determined at the time of the curve bend occurring on the *E*-curve. Potential decreases versus time in the second section (curves (6), (7), and (8), Fig. 2) was conditioned by a base depassivation.

3.3. Influence of charge- and discharge-current density

The properties of the lithium deposits and the efficiency of their cycling behaviour depend on the value of charge-current density and, in the common case, on the relation between charge-current density and deposit dissolution. Fig. 3 compares the data concerning the influence of charge-current density on the impedance characteristics of lithium deposits. The curves of Fig. 3(b) correspond to the deposition at a current density of 0.05 mA/cm^2 (0.06 mA). The curves presented in

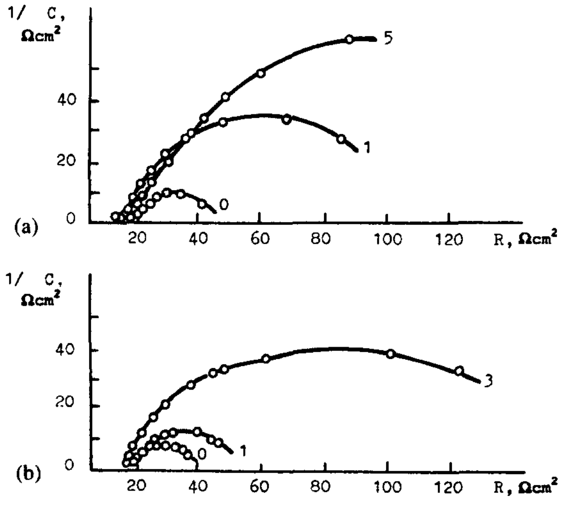

Fig. 3. Charge-current density vs. impedance characteristics of lithium deposit. Electrolyte: 1 M LiAsF$_6$, 2-methyltetrahydrofuran–tetrahydrofuran. Figures on the curves indicate the time of deposit passivation (24 h). (a) Charge current = 0.5 mA/cm^2, and deposition time = 2 h. (b) Charge current = 1 cm^2, and deposition time = 1 h.

Fig. 3(a) were obtained at a charge-current density of 1 mA/cm^2 (0.12 mA). The quantity of electricity was the same – 1 mAh/cm^2 – in both cases. It is evident that the deposition obtained at a lower current density has a greater resistance. This can be conditioned by the fact that the surface of freshly deposited lithium contacts the electrolyte to a greater extent and is stronger passivated at deposition by a lower current. The properties of the primary passivating film obtained under such conditions determine the deposit behaviour at its 'ageing': the resistance of the passivating film decreases at increasing charge-current density.

The parameters of the passivating film on the lithium deposits are determined by the ratio of lithium deposition rate versus its passivation rate.

Fig. 4 shows the effect of charge-current density on the character of charge/discharge curves of the anode based on a lithium–aluminium alloy. It is clear that at a charge current increasing from 0.5 to 2 mA/cm^2 the efficiency of deposit rises from 79 to 94%.

In the case of an Li–Al alloy at charge-current density increasing the efficiency of the anodic dissolution of deposit has a maximum in the 5–7 mA/cm^2 region (Fig. 5). It is evident, as far as in the range of high current densities, porous deposits having a low electrochemical efficiency begin to form. The nature of the effect of the current density depends on the alloy composition. Cycling efficiency of a lithium–boron alloy is low and almost independent of the current density.

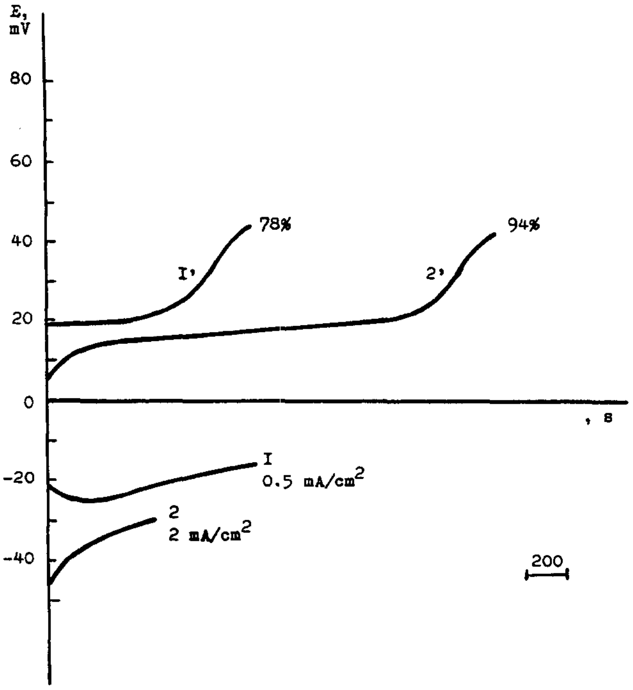

Fig. 4. Charge current density vs. cycling efficiency of anode of the lithium–aluminium alloy. Electrolyte: 1 M $LiBF_4$, propylene carbonate–dimethyl ether of diethyleneglycol (1:1). Discharge current = 0.5 mA/cm^2. Figures on the curves indicate the cycling efficiency of lithium deposit.

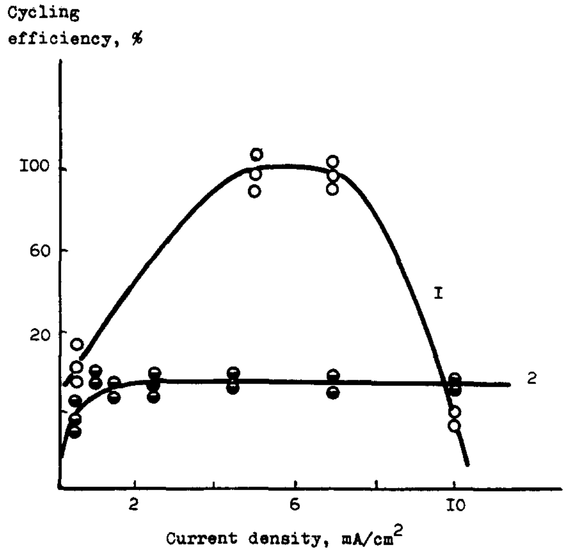

Fig. 5. Discharge current density vs. cycling efficiency of lithium deposits. (1) Electrolyte: 1 M $LiAsF_6$, 2-methyltetrahydrofuran–tetrahydrofuran; electrode: lithium–aluminium alloy; $i_{dis.} = i_{dep.}$. (2) Electrolyte: 1 M $LiBF_4$, propylene carbonate, dimethyl ether of diethyleneglycol; electrode: lithium–boron alloy; $i_{dis.} = 0.5$ mA/cm^2.

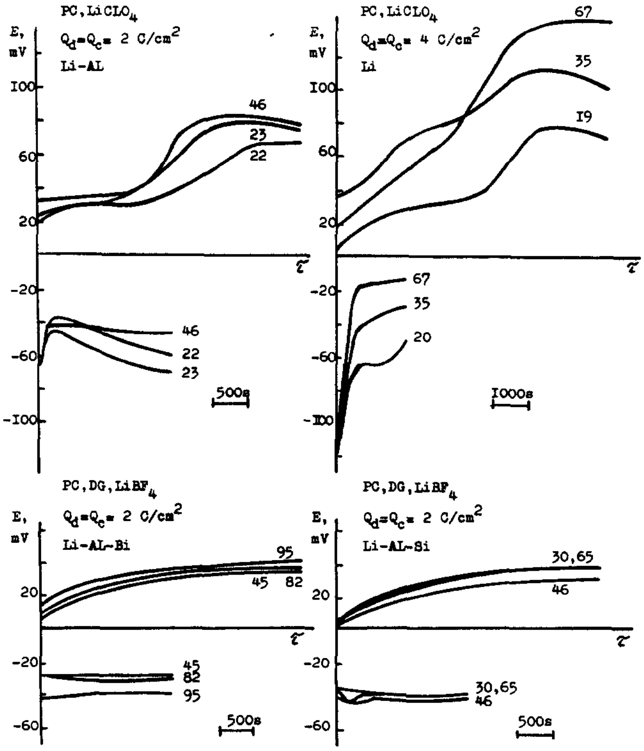

Fig. 6. Potential change at cycling during lithium dissolution and deposition on different bases. Figures on curves correspond to the cycle number.

Fig. 6 compares the curves of lithium deposit dissolution at various currents. It is clear that at a decreasing discharge current cycling efficiency increases significantly. The value of discharge current has a greater effect than the level of base passivation (see curves (6) and (7)).

3.4. Effect of the alloy composition on the cycling efficiency

The data cited above show the dependence of cycling efficiency on the passivation level of the anode surface. In this case, a correlation has been observed: the efficiency of galvanostatic cycling is higher when active component of anode/electrolyte boundary impedance is lower. These conclusions are confirmed by the comparison of cycling efficiency of lithium–aluminium alloys with various compositions.

Table 2 shows the maximum cycling efficiency of an alloy with a 5 mass% Al content. The anode based on this alloy is passivated to a lesser extent (Fig. 1, Table 1). The alloy with 16.8 mass% Al has a minimum cycling efficiency. The anode based on this alloy is passivated to a greater extent (Fig. 1, Table 1).

Alloy compositions affect to a great extent the dynamics of the process of lithium deposition/dissolution. Thus, comparatively low polarization of cathode and anode processes is the peculiarity of electrochemical behaviour of ternary alloys of Li–Al–Cd, Li–Al–Bi, Li–Al–Si. In alloys with the addition of bismuth and silicon, the curve bend is absent on the E–τ curve of deposit dissolution, i.e., there is no difference between the potentials of deposit dissolution and base dissolution (Fig. 6). This system behaves as a one-phase one. This can be conditioned by the binary alloy passivation in the electrolyte.

Table 2
Influence of lithium–aluminium alloys on cycling efficiency in free electrolyte: propylene carbonyl, DG, $LiBF_4$, $i = 0.5$ mA/cm^2

Alloy composition	i (mA/cm^2)	Cycling efficiency (%)
Lithium–aluminium alloy, 5 mass% Al	0.5	78
	2.0	94
	3.0	97
Lithium–aluminium alloy, 16.8 mass% Al	0.5	55
	2.0	73
Lithium–aluminium alloy, 22.5 mass% Al	0.5	60
	2.0	70

4. Conclusions

1. In a series of lithium, binary lithium–aluminium alloys, ternary alloys of lithium–aluminium with addition of silicon, bismuth or cadmium, surface passivation decreases in a non-aqueous electrolyte.
2. The resistance of the passivating film reaches a maximum by increasing the aluminium content in the alloy.
3. The efficiency of lithium depositions increases a decreasing resistance of the passivating film.
4. At the electrochemical deposition of lithium the level of passivation of the deposit and the efficiency of its anodic dissolution is determined by the ratio of electrochemical deposition rate and the rate of passivation. The efficiency of the anode cycling passes through a maximum by increasing charge-current density. Cycling efficiency rises when discharge current density is decreasing.
5. Lithium insertion into the structure of ternary alloys proceeds easier at its electrochemical deposition than into the structure of lithium or binary Li–Al alloy.

Acknowledgements

The financial support from Chemical Concentrates Plant, Novosibirsk, Russian Federation is greatly acknowledged.

References

[1] S. Atsusy, I. Sigery and I. Kenjity, *Jpn. Patent No. 62 139 276* (1985).
[2] N. Hidenory, S. Tosikadsy and K. Hirosy, *Jpn. Patent No. 62 147 656* (1985).
[3] K. Nobuharu, I. Toshiko and T. Kentjity, *Jpn. Patent No. 63 266 346* (1988).
[4] S. Hiroyuki, F. Kadzunori, M. Mamoro, M. Atsuko and E. Noboru, *Jpn. Patent No. 61 282 956* (1986).
[5] O. Akira, Y. Yosima, Y. Ken and K. Tecuro, *Jpn. Patent No. 61 281 784* (1986).
[6] J.O. Besenhard, M. Hess and P. Komenda, *Solid State Ionics, 40* (1990) 525–529.
[7] E.M. Shembel, O.S. Ksenzhek and I.M. Maksyuta, *Elektrokhimiya, 22* (1986) 446–451.
[8] E.M. Shembel, I.M. Maksyuta and O.S. Ksenzhek, *Elektrokhimiya, 23* (1987) 701–704.